2022 IEEE 61st Conference on Decision and Control (CDC)
December 6-9, 2022. Cancún, Mexico

A Tutorial on Pontryagin-Koopman Operators for Infinite Horizon Optimal Control

Yuxuan Guo[1], Boris Houska[1], Mario E. Villanueva[1,2]

Abstract— **This paper provides a tutorial on how to use Koopman operators to lift Pontryagin's optimality condition for infinite-horizon optimal control problems into an infinite dimensional space. It is shown how to exploit the symplectic structure of the associated Pontryagin-Koopman operator in order to identify the stable manifold on which optimal trajectories evolve. Moreover, it is shown how to conduct a Koopman mode analysis in order to characterize optimal feedback control laws. Our focus is on providing a review of and gain further insight into the theory of Koopman-operator based optimal control methods. This is achieved by exploiting the structure of a particular optimal regulation problem, which is used as a tutorial example throughout the paper.**

I. Introduction

The last decade has witnessed a growing interest in the use of Koopman operator theory [5] in different areas of time-autonomous dynamic system analysis [9], [10]. It is, however, only a very recent observation that Koopman operators might also be useful in the context of control system analysis and method development [6]. In this context, it should be mentioned that Koopman's formalism cannot be applied directly to systems with time-varying control inputs, as a Koopman mode analysis is usually only accurate for analyzing time-autonomous systems. Nevertheless, in the context of optimal control of autonomous systems, one can apply Koopman's formalism to Pontryagin's differential equations [12], which—at least in the simplest setting—have no explicit time dependence.

The goal of the present paper is to present a tutorial, discussion, and interpretation of the results in [12], which lead to new insight on how to construct global solutions of nonlinear control problems by using a Koopman mode analysis. In order to understand the relevance of this line of research, one needs to be aware of the fact that there exist various approaches for global optimal control—each with their advantages and disadvantages. For example, one can take a direct route and attempt to parameterize the control input and apply a branch-and-bound scheme on the space of parameterization coefficients [3]. This approach is—due the curse of dimensionality—limited to low dimensional input parameterizations. An alternative is provided by branch-and-lift schemes, which branch over projections of the controls over subspaces of increasing dimension instead of directly discretizing the control variables—potentially alleviating the memory cost associated to branch-and-bound schemes [4].

*This work was supported by
[1]ShanghaiTech University, Shanghai, China
[2]IMT School for Advanced Studies Lucca, Lucca, Italy

Apart from branching-based enumeration methods, one can search for viscosity solutions of Hamilton-Jacobi-Bellman (HJB) partial differential equations from which globally optimal controllers can be constructed [2], [1]. These approaches are, however, limited to problems with a small number of states due to the worst-case exponential cost of back-propagating the value function in the state space. Last but not least, yet another option for globally optimal control synthesis is to reformulate the optimal control problem in a higher dimensional space. This may reveal structures that facilitate the solving process. For example, [7] considers lifting optimal control problems into an infinite dimensional space by means of occupation measures, where the problem becomes a linear program. This infinite-dimensional LP can then be solved using a hierarchy of linear matrix inequalities.

Contribution

The main contribution of the current paper consists of an explicit tutorial example, visualization, and interpretation of a global optimal control method that has originally been published in [12]. For this aim, Section II introduces time-autonomous optimal infinite-horizon optimal control problems, the main technical assumptions, and a non-trivial tutorial optimal control problem that shall be solved explicitly by using the methods that are reviewed in this paper. Sections III, IV, V, and VI start each with a brief review of, respectively, Pontryagin's differential equation, its symplectic structure, Pontryagin-Koopman operators and their spectrum, as well as the final mode analysis that can be used to construct globally optimal feedback controllers. The short theory reviews of all these sections are all visualized and discussed by revisiting our guiding tutorial example multiple times. Notice that the corresponding explicit strategies for solving this tutorial are not trivial at all—see Lemma 1, Proposition 1, as well as Theorems 1 and 2. These results are actual technical contributions of this paper, whose interpretations help to gain novel insight into Pontyagin-Koopman operator theory. Finally, Section VII concludes the paper by highlighting the relevance of these technical insights in the context of developing future methods for global optimal control.

Notation

The set of square integrable function, $\phi : \mathbb{R}^n \to \mathbb{C}$, is denoted by $\mathbb{L}^n_2$. The symbol $\mathbb{W}^n_{2,2}$ denotes the Sobolev space of functions which are twice weakly-differentiable on $\mathbb{R}^n$ and whose weak derivatives up to second order are in $\mathbb{L}^n_2$.

978-1-6654-6761-2/22/$31.00 ©2022 IEEE

The gradient operator is denoted by ∇. The symbol I is used to denote an identity matrix of appropriate dimension.

II. Infinite Horizon Control

This paper is concerned with infinite-horizon optimal control problems

$$V(x_0) = \min_{x,u} \int_0^\infty \ell(x(t), u(t))\mathrm{d}t \quad \text{s.t.} \quad \begin{cases} \forall t \in [0,\infty) \\ \dot{x}(t) = f(x(t), u(t)) \\ x(0) = x_0 \ , \end{cases} \tag{1}$$

with the initial condition $x_0 \in \mathbb{R}^{n_x}$ assumed to be given. Here, $x(t) \in \mathbb{R}^{n_x}$ and $u(t) \in \mathbb{R}^{n_u}$ denote the state and control vectors at time $t \in [0,\infty)$, respectively. An optimal infinite-horizon feedback law $\mu^\star : \mathbb{R}^{n_x} \to \mathbb{R}^{n_u}$ is regular, if the trajectory $(x^\star, u^\star)$ with $u^\star(t) = \mu^\star(x^\star(t))$ is a minimizer of (1) and converges to a steady state $(x_\mathrm{s}, u_\mathrm{s})$ with $u_\mathrm{s} = \mu^\star(x_\mathrm{s})$.

The following blanket assumptions, which have been slightly simplified with respect to those in [12], are imposed throughout the remainder of this paper.

- **A1** The right-hand side function $f : \mathbb{R}^{n_x} \times \mathbb{R}^{n_u} \to \mathbb{R}^{n_x}$ is twice-continuously differentiable, globally Lipschitz continuous in x, and affine in u.
- **A2** The cost function $\ell : \mathbb{R}^{n_x} \times \mathbb{R}^{n_u} \to \mathbb{R}_+$ is twice continuously differentiable and strongly convex in u.
- **A3** Any steady-state $(x_\mathrm{s}, u_\mathrm{s})$ corresponding to the optimal solution $(x^\star(t), u^\star(t))$ satisfies
$$f(x_\mathrm{s}, u_\mathrm{s}) = 0 \quad \text{and} \quad \ell(x_\mathrm{s}, u_\mathrm{s}) = 0 \ .$$
- **A4** The Algebraic Riccati equation
$$0 = PA + A^\mathsf{T}P + Q - (PB + S)R^{-1}(PB + S)^\mathsf{T} \ ,$$
admits a positive definite solution $P \succeq 0$, assuming that all derivatives, $A = \nabla_x f$, $B = \nabla_u f$, $Q = \nabla^2_{xx}\ell$, $R = \nabla^2_{uu}\ell$, and $S = \nabla_{xu}\ell$ are evaluated at the steady-state $(x_\mathrm{s}, u_\mathrm{s})$.

Notice that **A3** and **A4**, ensure that the parametric value function $V(x_0)$ remains finite, whenever (1) is feasible [8].

A. Tutorial Example I: Problem Setting

Throughout this paper, we study the tutorial optimal control problem

$$V(x_0) = \min_{x,u} \int_0^\infty \left(x^2(t) + u^2(t)\right) \mathrm{d}t \quad \text{s.t.} \quad \begin{cases} \forall t \in [0,\infty) \\ \dot{x}(t) = -x^3(t) + u(t) \\ x(0) = x_0 \ . \end{cases} \tag{2}$$

This problem has the globally optimal feedback control law

$$\mu^\star(x) = x^3 - x\sqrt{1 + x^4},$$

which stabilizes the system at the origin. In the sections below, we will use a Koopman-operator approach in order to verify this solution.

III. Pontryagin's Maximum Principle

This section briefly reviews Pontryagin's Maximum Principle (PMP) [11] for (1). Let $H : \mathbb{R}^{n_x} \times \mathbb{R}^{n_u} \times \mathbb{R}^{n_x} \to \mathbb{R}$ denote the Hamiltonian, given by

$$H(x, u, \lambda) = \lambda^\mathsf{T} f(x, u) + \ell(x, u) \tag{3}$$

with $\lambda \in \mathbb{R}^{n_x}$. Since f and ℓ are, per assumptions **A1** and **A2**, twice continuously differentiable, H is twice continuously differentiable, too, and the parametric minimizer

$$u^\star(x, \lambda) \in \operatorname*{argmin}_u \ H(x, u, \lambda) \tag{4}$$

is unique. Next, the PMP states that any optimal solution (x, u) of (1) necessarily satisfies the ODE system

$$\dot{y}(t) = F(y(t)) \quad \text{with} \quad F(y(t)) = \begin{pmatrix} \nabla_\lambda H^\star(x(t), \lambda(t)) \\ -\nabla_x H^\star(x(t), \lambda(t)) \end{pmatrix} \tag{5}$$

for a costate function $\lambda \in \mathbb{W}^{n_x}_{2,2}$. Here, we have introduced the stacked state $y = [x^\mathsf{T}, \lambda^\mathsf{T}]^\mathsf{T}$ and the reduced Hamiltonian

$$H^\star(x, \lambda) = H(x, u^\star(x, \lambda), \lambda) \ .$$

Besides Pontryagin's ODE, minimizers of (1), must satisfy necessary boundary conditions. This includes the initial value condition $x(0) = x_0$ and the limit condition

$$\lim_{t\to\infty} \lambda(t) = 0,$$

due to Assumptions **A1**-**A4**.

A. Tutorial Example II: Pontryagin's ODEs

The reduced Hamiltonian for our example is given by

$$H^\star(x, \lambda) = -\lambda x^3 - \frac{\lambda^2}{4} + x^2 \ . \tag{6}$$

Thus, Pontryagin's differential equations for (2) are

$$\begin{aligned} \dot{x}(t) &= -x^3(t) - \frac{\lambda(t)}{2} \\ \dot{\lambda}(t) &= -2x(t) + 3x^2(t)\lambda(t) \ , \end{aligned} \tag{7}$$

with boundary conditions

$$x(0) = x_0 \quad \text{and} \quad \lim_{t\to\infty} \ \lambda(t) = 0 \ .$$

IV. Symplectic Structure of Pontryagin Flows

Let Γ_t denote the flow of (5) in the phase space $\mathbb{R}^{2n_x}$, which satisfies

$$\forall y \in \mathbb{R}^{2n_x}, \quad \frac{\mathrm{d}}{\mathrm{d}t}\Gamma_t(y) = F(\Gamma_t(y)) \ \text{ and } \ \Gamma_0(y) = y \ . \tag{8}$$

Assumptions **A1**, **A2**, **A3** guarantee that Γ_t is a well-defined continuously differentiable function. By writing the vector field of Pontryagin's ODE in the form

$$F(y) = \Omega\nabla H^\star(y) \quad \text{with} \quad \Omega = \begin{bmatrix} 0 & I \\ -I & 0 \end{bmatrix}, \tag{9}$$

Γ_t can be shown to be a symplectic flow in the symplectic space $(\mathbb{R}^{2n_x}, \Omega)$. Some properties related to symplecticity

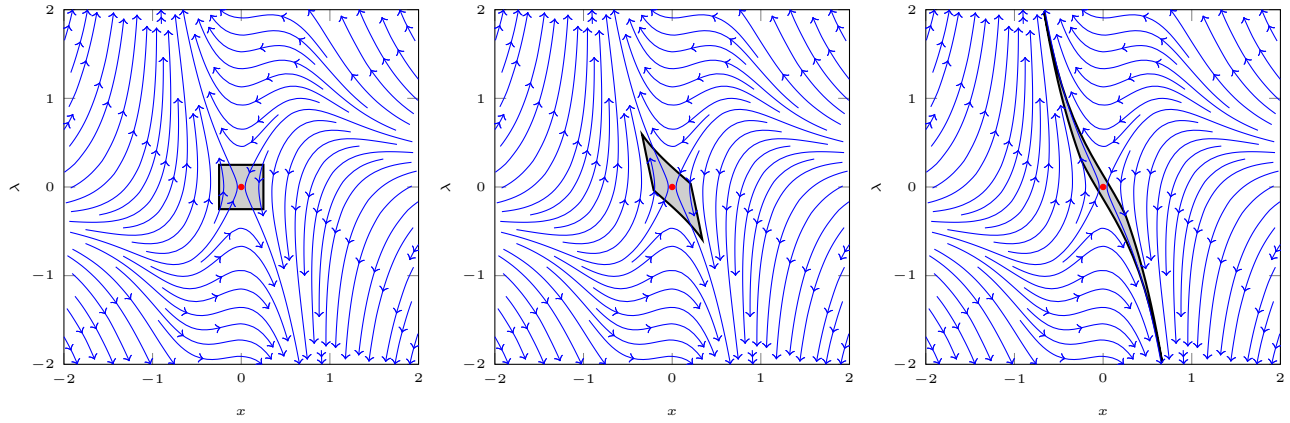

Fig. 1. Action of the flow Γ_t on the set Y_0 for $t = 0$ (left), $t = 0.5$ (middle), and $t = 1.25$ (right). The set $\Gamma_t(X_0)$ is shown in gray with black boundary. The red point corresponds to the optimal steady-state. The flow of the vector field F is visualized by the blue arrows.

are revealed in [12]. For example, the Hamiltonian $H^\star$ is invariant for the symplectic flow, since

$$\begin{aligned}\frac{\mathrm{d}}{\mathrm{d}t}\left(H^\star \circ \Gamma_t\right) &= \left(\nabla H^\star \circ \Gamma_t\right)^\intercal \left(\frac{\mathrm{d}}{\mathrm{d}t}\Gamma_t(y)\right) \\ &= \left(\nabla H^\star \circ \Gamma_t\right)^\intercal \Omega \left(\nabla H^\star \circ \Gamma_t\right) = 0\,.\end{aligned}$$

In addition, the vector field F is divergence-free, or equivalently, the symplectic flow Γ_t is volume-preserving, that is

$$\forall t \in \mathbb{R}, \quad \det\left(\frac{\partial}{\partial y}\Gamma_t\right) = 1\,,$$

which means the volume of any set is invariant along the flow Γ_t.

A. Tutorial Example III: Symplecticity of the Flow Γ_t

The properties of symplectic flows can be understood by revisiting our tutorial example. For instance, let us consider the set $Y_0 = [-\frac{1}{4}, \frac{1}{4}] \times [-\frac{1}{4}, \frac{1}{4}]$ with area $\frac{1}{4}$. Figure 1 shows the set Y_0 under the action of the flow Γ_t for the time points $t \in \{0.0, 0.5, 1.25\}$. Notice that as the time increases, the set $\Gamma_t(Y_0) = \{\Gamma_t(y) | y \in Y_0\}$ gets deformed, with the left corners being pulled by the flow upwards and the right corners downwards. However, the area of each of these sets $\Gamma_t(Y_0)$ remains invariant with a value of $\frac{1}{4}$. Figure 2 illustrates level sets of $H^\star$ (red lines), which remain invariant along the flow (blue lines). Back to the OCP (2) and Pontryagin's ODE (7), the invariant relation implies the zero level set of $H^\star$ contains the optimal steady-state 0.

V. Pontryagin-Koopman Operators and Their Spectral Properties

An interesting path towards further analyzing and solving Pontryagin's optimality condition proceeds by introducing the Pontryagin-Koopman operator, $U_t : \mathbb{W}^{2n_x}_{2,2} \to \mathbb{W}^{2n_x}_{2,2}$, with

$$\forall \varphi \in \mathbb{W}^{2n_x}_{2,2}, \quad U_t\varphi \stackrel{\text{def}}{=} \varphi \circ \Gamma_t.$$

That is, U_t is an element of the one-parameter unitary group of Koopman operators associated to the flow Γ_t of Pontryagin's ODE system (5). Pontryagin-Koopman operators are—as any other Koopman operator—invertible and linear.

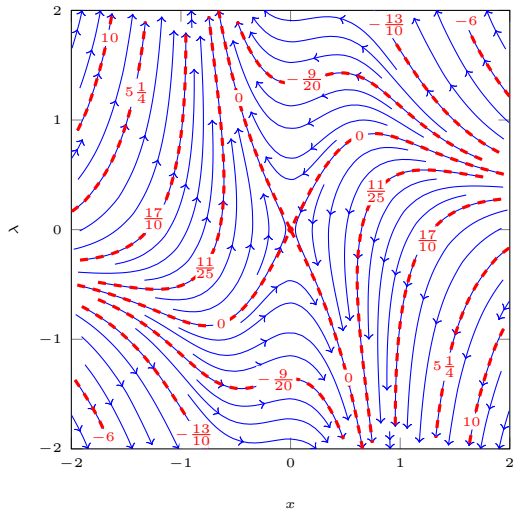

Fig. 2. The Pontryagin flow (blue lines) and selected level sets of the reduced Hamiltonian function $H^\star$ (red lines).

Instead of directly analyzing U_t, one can take an alternative route by defining its associated differential Pontryagin-Koopman operator L as

$$\forall \varphi \in \mathbb{W}^{2n_x}_{2,2}, \quad L\varphi \stackrel{\text{def}}{=} F^\intercal \nabla \varphi\,.$$

Notice that we have $L = \dot{U}_t|_{t=0}$. Thus, the Koopman operator is the exponential of L, that is $U_t = e^{tL}$.

Definition 1: A function $\Psi_\kappa \in \mathbb{W}^{2n_x}_{2,2}$ is an eigenfunction of L with eigenvalue $\kappa \in \mathbb{C}$ if it satisfies

$$L\Psi_\kappa = \kappa\Psi_\kappa\,. \tag{10}$$

Here, we also have the relation

$$U_t\Psi_\kappa = e^{tL}\Psi_\kappa = e^{\kappa t}\Psi_\kappa$$

so Ψ_κ is also said to be an eigenfunction of the Koopman operator U_t with eigenvalue $e^{\kappa t}$ [10]. Notice that L is a linear operator too. Therefore, the relation in (10) can be equivalently written as the linear partial differential equation,

$$F^\intercal \nabla \Psi_\kappa = \kappa\Psi_\kappa\,, \tag{11}$$

also called the Pontryagin-Koopman PDE of (1). The spectral properties of generic Koopman operators are connected to the structural properties of a dynamic system. It may be not too surprising, that Pontryagin-Koopman operators possess a symplectic structure—inherited from the symplecticity of the associated Pontryagin flow, and that this structure induces a particular structure in the spectrum of these operators. In light of this observation, and as further elaborated in [12], this symplectic structure allows us to make the following statement about the existence of eigenvalues and eigenfunctions of the differential Pontryagin-Koopman operator L.

Theorem 1: Let Assumptions **A1**, **A2**, and **A3** be satisfied. Suppose that the matrix $\nabla F(x_\mathrm{s}, \lambda_\mathrm{s})$ is diagonalizable. Then, there exist at least $2n_x$ complex eigenvalues

$$\kappa_1, \ldots, \kappa_{n_x}, \kappa'_1, \ldots, \kappa'_{n_x} \in \sigma(L)$$

such that $\kappa_i = -\kappa'_i$ for all $i \in \{1, \ldots, n_x\}$.

This theorem, whose proof can be found in [12, Corollary 2 and Remark 4] combined with [9, Proposition 2], asserts that the spectrum of Pontryagin-Koopman operators possesses at least $2n_x$ mirrored eigenvalues.

A. Example IV: Insights from the Method of Characteristics

Let us come back to our tutorial example in order to explain how the method of characteristics can be used to construct eigenfunctions of Pontryagin-Koopman operators. For this aim, we need to introduce a non-recurrent set.

Definition 2: A set $\mathcal{S} \subseteq \mathbb{R}^{2n_x}$ is called a non-recurrent set of Γ_t, if $\Gamma_t(y) \notin \mathcal{S}$ for all $y \in \mathcal{S}$ and all $t > 0$.

In the following, we partition the phase space as

$$\mathbb{R}^2 = \mathcal{H}_- \cup \mathcal{H}_+ \cup \mathcal{H}_0 \,, \quad \begin{cases} \mathcal{H}_- = \{(x,\lambda) \,|\, H^\star(x,\lambda) < 0\} \\ \mathcal{H}_+ = \{(x,\lambda) \,|\, H^\star(x,\lambda) > 0\} \\ \mathcal{H}_0 = \{(x,\lambda) \,|\, H^\star(x,\lambda) = 0\} \,. \end{cases}$$

Moreover, we introduce the set

$$\mathcal{S} = \left\{(x,\lambda) \in \mathbb{R}^2 \;\middle|\; x\lambda = 0\right\} \setminus \{(0,0)\} \,. \tag{12}$$

Lemma 1: Let Γ_t be the flow of (5). The set $\mathcal{S}$ is non-recurrent for Γ_t for all $t \in \mathbb{R}$ and $\forall (x,\lambda) \in \mathcal{H}_+ \cup \mathcal{H}_-$, there exists a time $t_S \in \mathbb{R}$ such that

$$S(x,\lambda) \stackrel{\text{def}}{=} \Gamma_{-t_S}(x,\lambda) \in \mathcal{S} \,.$$

Proof: Since $H^\star$ is an invariant of the Pontryagin flow, the set $\mathcal{H}_-$ is, by construction, an invariant set. In particular, if $(x,\lambda) \in \mathcal{H}_-$ then $\Gamma_t(x,\lambda) \notin \{(x,0) \,|\, x \in \mathbb{R}\}$ for all $t \in \mathbb{R}$, since $H^\star(x,0) = x^2 > 0$ for all $x \in \mathbb{R}$. Let the function $V_- : \mathcal{H}_- \to \mathbb{R}$ be defined as $V_-(x,\lambda) = x^3\lambda$. The zero level set of this function is the λ-axis. Because we have

$$\frac{\mathrm{d}}{\mathrm{d}t} V_-(x(t),\lambda(t)) = -\left(2x(t)^4 + \frac{3}{2}x(t)^2\lambda(t)^2\right) < 0$$

whenever $x(t) \neq 0$ the function V_- is monotonically decreasing along the trajectories of the system. Together with uniqueness of solutions for (7), these arguments imply that the trajectories of the system evolving in $\mathcal{H}_-$ will touch $\mathcal{S}$ only once—somewhere on the λ-axis. A similar analysis can be carried out by using the function $V_+ : \mathcal{H}_+ \to \mathbb{R}$ with $V_+(x,\lambda) = x\lambda^{\frac{1}{3}}$ to conclude that the trajectories evolving on the invariant set H_+ will touch $\mathcal{S}$ once, somewhere on the x-axis. ■

The following proposition uses the method of characteristic to explicitly construct eigenfunction of the Pontryagin-Koopman operator for our tutorial example.

Proposition 1: Suppose $g \in \mathbb{W}^2_{2,2}$ is any complex-valued function defined on $\mathcal{S}$. There exists a function $\tau : \mathbb{R}^2 \to \mathbb{R}$ such that for any $\kappa \in \mathbb{C}$, the function $\Psi_\kappa : \mathbb{R}^2 \to \mathbb{C}$ with

$$\Psi_\kappa(x,\lambda) = g(S(x,\lambda))e^{\kappa\tau(x,\lambda)}$$

is an eigenfunction of the Pontryagin-Koopman operator for the flow associated to (7).

Proof: See Appendix A for a proof. ■

The proof of this proposition constructively shows that the map τ—representing the backwards flow time from $\mathcal{S}$ to any point in $\mathbb{R}^2$ is given by

$$\tau(x,\lambda) = \begin{cases} \eta_+ G(m(s),k)\big|^x_{\mathrm{sgn}(x)\sqrt{H^\star(x,\lambda)}} & \text{if } (x,\lambda) \in \mathcal{H}_+ \\ \eta_- G(m(x),k) & \text{if } (x,\lambda) \in \mathcal{H}_- \\ \eta_0 \lim\limits_{a\to 0} \coth^{-1}\left(\sqrt{s^4+1}\right)\Big|^x_a & \text{otherwise} \,. \end{cases}$$

Here, $G : \mathbb{R} \times (0,1) \to \mathbb{C}$ denotes the elliptic integral of the first kind[1], whose argument and parameter are, respectively

$$m(s) = \arcsin\left(\frac{s\sqrt{\beta-\alpha}}{\sqrt{\beta(s^2-\alpha)}}\right) \quad \text{and} \quad k = \frac{\beta(\alpha-\gamma)}{\gamma(\alpha-\beta)} \,.$$

Moreover, we have defined the shorthands

$$\eta_\pm = \pm\frac{\mathrm{sgn}(\lambda+2x^3)}{\sqrt{\gamma(\beta-\alpha)}} \quad \text{and} \quad \eta_0 = \frac{\mathrm{sgn}(x\lambda)}{2}$$

with $\alpha \in \mathbb{R}$ and $\beta, \gamma \in \mathbb{C}$ denoting the roots of the cubic equation

$$s^3 + s - H^\star(x,\lambda) = 0 \,.$$

A few remarks are in order. First, notice that Theorem 1 states that Koopman-Pontryagin operators have at least $2n_x$ mirrored eigenvalues. In Proposition 1, we have established the existence of infinitely many mirrored eigenvalues, since κ is arbitrary. Furthermore, one could compute explicitly the flow map Γ_t, since the elliptic functions in τ can be inverted by means of the Jacobi amplitude function. Since this is cumbersome and does not yield useful additional insight, we focus instead on computing the limit values of the eigenfunctions. For example, consider an eigenfunction for $\kappa \in \mathbb{C}$ with $\mathrm{Re}(\kappa) > 0$. The construction from the above propositions implies that

$$\Psi_\kappa(x,\lambda) = \begin{cases} 0 & \text{if } \mathrm{sgn}(x\lambda) = 1 \\ \infty & \text{otherwise} \,, \end{cases}$$

[1]The elliptic integral of the first kind $G : \mathbb{R} \times (0,1) \to \mathbb{C}$ is given by

$$G(\phi,k) = \int_0^\phi \frac{\mathrm{d}\theta}{\sqrt{1-k\sin^2(\theta)}} \,.$$

for all (x, λ) such that $H^\star(x, \lambda) = 0$. Of course, an inverse statement can be obtained for the mirrored eigenvalues $-\kappa$. As we shall see next, this information is all we need for our ultimate purpose of constructing globally optimal feedback laws for (2).

VI. Characterization of Optimal Feedback Controls

This section shows how to use the above reviewed Koopman operator to solve (1) explicitly. The following theorem summarizes a simplified version of Theorem 3 in [12], which establishes the fact that regular optimal solutions of (1) evolve on the manifold of unstable Pontryagin-Koopman eigenfunctions

$$\mathcal{M}_+ = \left\{(x, \lambda) \in \mathbb{R}^{2n_x} \,|\, \forall \kappa \in \sigma_+(L) : \Psi_\kappa(x, \lambda) = 0\right\}.$$

Here, $\sigma_+(L)$ denotes the set of *unstable* eigenvalues

$$\sigma_+(L) = \{\kappa \in \sigma(L) \mid \mathrm{Re}(\kappa) > 0\} \ .$$

Theorem 2: Let Assumptions **A1**-**A4** hold and let $\mu^\star : \mathbb{R}^{n_x} \to \mathbb{R}^{n_u}$ be a regular optimal control law for the infinite-horizon OCP (1). Then, there exists a function $\Lambda : \mathbb{R}^{n_x} \to \mathbb{R}^{n_x}$ such that

$$(x, \Lambda(x)) \in \mathcal{M}_+ \quad \text{and} \quad \mu^\star(x) = u^\star(x, \Lambda(x)) \ .$$

Theorem 2, together with Theorem 1 regarding the spectral properties of the Pontryagin-Koopman operator, provides a means to systematically search for solutions of (1). This is achieved by solving the equation system

$$\Psi_\kappa(x, \lambda) = 0$$

which has the globally optimal solution of (1) corresponding to one of the finite number of parametric solutions $\lambda = \Lambda(x)$. The details of this methodology can be found in [12].

A. Example V: Exact Optimal Solution

Recall that we have already showed that for points (x, λ) for which $H^\star(x, \lambda) = 0$ satisfy $\Psi_\kappa(x, \lambda) = 0$, whenever $\mathrm{sgn}(x\lambda) = 1$ and $\mathrm{Re}(\kappa) > 0$. Therefore, we arrive at an explicit representation of our unstable manifold,

$$\mathcal{M}_+ = \left\{ (x, \lambda) \;\middle|\; \begin{array}{c} -x^3\lambda + x^2 - \frac{1}{4}\lambda^2 = 0 \\ \text{and} \quad \mathrm{sgn}(x\lambda) = 1 \end{array} \right\} . \tag{13}$$

We have a single nonlinear equation, which can be solved and simplified— using the condition $\mathrm{sgn}(x\lambda) = 1$—to

$$\Lambda(x) = 2\left(-x^3 + x\sqrt{x^4 + 1}\right) \ . \tag{14}$$

By substituting this relation into our expression for the parametric minimizer of the Hamiltonian, we indeed recover the optimal feedback law

$$\mu^\star(x) = u^\star(x, \Lambda(x)) = -\frac{\Lambda(x)}{2} = x^3 - x\sqrt{x^4 + 1} \ . \tag{15}$$

Figure 3 shows the manifold of unstable Koopman eigenfunctions $\mathcal{M}_+$ as a red dashed line together with the flow of (7). Notice that $\mathcal{M}_+$ corresponds to the stable manifold of the system—which is the key point of Theorem 2. This also corresponds to the zero level set of the reduced Hamiltonian, which should be expected as it is the only contour line that includes the optimal steady-state. Notice also Λ maps any point x_0 to its associate image $(x_0, \Lambda(x_0)) \in \mathcal{M}_+$. Since the Hamiltonian is constant along the solutions of (7) any such point will flow towards the origin as time goes to infinity.

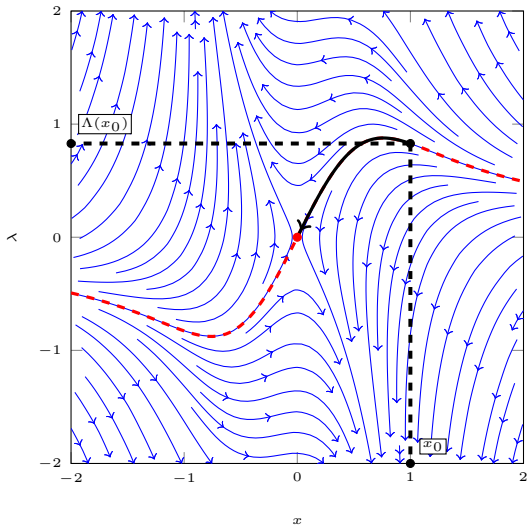

Fig. 3. The stable manifold for the (7) corresponds to $\mathcal{M}_+$ (dashed red line). A sample trajectory for a given x_0 is shown as a black arrow.

Throughout the previous sections we described the main concepts for analyzing infinite-horizon optimal control problems by means of Pontryagin-Koopman operator theory. In particular, we showed how to formulate the associated autonomous (Pontryagin) dynamic system as well as how to define its associated Pontryagin-Koopman operator by means of a linear partial differential equation. This PDE was then used to construct the eigenfunctions of the operator, which then were used to characterize the unstable manifold of the system and ultimately construct the globally optimal feedback law for the original infinite horizon optimal control problem. From a practical perspective, the key difficulty for applying the Pontryagin-Koopman operator approach is the solution of the PDE. For the particular example in this paper, the construction of the exact feedback law was possible since the associated PDE admits an analytical solution by means of the method of characteristics—a feat that is, more often than not, impossible. Nevertheless, we must point out that Pontryagin-Koopman PDEs are always linear and while an analytical solution may not be possible they are amenable to numerical solution using a large variety of numerical discretization schemes. This is in contrast to the alternative method of computing globally optimal feedback laws using HJB theory, which requires the solution of a nonlinear PDE.

To summarize, Pontryagin-Koopman operators not only provide a novel theoretical perspective for global optimal control, but also provide a direction towards the construction of scalable numerical algorithms for globally optimal synthesis.

VII. Conclusion

This paper has presented a tutorial-style review of the Pontryagin-Koopman operator theory from [12] for finding global solutions of optimal control problems. Our tutorial example has led to explicit insight on how to use this formalism on practical examples and, as such, this tutorial be viewed as an important preliminary step towards the development of completely novel types of global optimal control algorithms, although the details on how such algorithms could be constructed will be the subject to future work.

References

[1] M. Bardi, I. C. Dolcetta, et al. *Optimal control and viscosity solutions of Hamilton-Jacobi-Bellman equations*, volume 12. Springer, 1997.

[2] R. E. Bellman. *Dynamic Programming*. Princeton University Press, Princeton, 1957.

[3] B. Chachuat, A. B. Singer, and P. I. Barton. Global methods for dynamic optimization and mixed-integer dynamic optimization. *Industrial & Engineering Chemistry Research*, 45(25):8373–8392, 2006.

[4] B. Houska and B. Chachuat. Branch-and-lift algorithm for deterministic global optimization in nonlinear optimal control. *Journal of Optimization Theory and Applications*, 162(1):208–248, 2014.

[5] B. O. Koopman. Hamiltonian systems and transformation in hilbert space. *Proceedings of the national academy of sciences of the united states of america*, 17(5):315, 1931.

[6] M. Korda and I. Mezić. Linear predictors for nonlinear dynamical systems: Koopman operator meets model predictive control. *Automatica*, 93:149–160, 2018.

[7] J. B. Lasserre, D. Henrion, C. Prieur, and E. Trélat. Nonlinear optimal control via occupation measures and lmi-relaxations. *SIAM journal on control and optimization*, 47(4):1643–1666, 2008.

[8] D. Liberzon. *Calculus of Variations and Optimal Control Theory: A Concise Introduction*. Princeton University Press, 2012.

[9] A. Mauroy and I. Mezić. Global stability analysis using the eigenfunctions of the koopman operator. *IEEE Transactions on Automatic Control*, 61(11):3356–3369, 2016.

[10] I. Mezić. Spectral properties of dynamical systems, model reduction and decompositions. *Nonlinear Dynamics*, 41(1-3):309–325, 2005.

[11] L. Pontryagin, V. Boltyanskii, R. Gamkrelidze, and E. Mishchenko. *The mathematical theory of optimal processes*. John Wiley & Sons, New York, 1962.

[12] M. E. Villanueva, C. Jones, and B. Houska. Towards global optimal control via koopman lifts. *Automatica*, 132:109610, 2021.

Appendix A: Proof of Proposition 1

Proof: The proof follows from solving

$$\left(-x^3-\frac{\lambda}{2}\right)\frac{\partial}{\partial x}\Psi_\kappa+\left(-2x+3x^2\lambda\right)\frac{\partial}{\partial\lambda}\Psi_\kappa=\kappa\Psi_\kappa \quad (16)$$

with the initial data $g:\mathcal{S}\to\mathbb{C}$.

The characteristic curves for (16) satisfy

$$\begin{aligned}\frac{\mathrm{d}}{\mathrm{d}\tau}x(\tau) &= -x(\tau)^3-\frac{1}{2}\lambda(\tau)\\ \frac{\mathrm{d}}{\mathrm{d}\tau}\lambda(\tau) &= -2x(\tau)+3x(\tau)^2\lambda(\tau)\\ \frac{\mathrm{d}}{\mathrm{d}\tau}\Psi_\kappa(\tau) &= \kappa\Psi_\kappa(\tau)\end{aligned} \quad (17)$$

with $\tau\in\mathbb{R}$ being the parameter. The last equation, yields

$$\Psi_\kappa(\tau)=e^{\kappa\tau}g(x_0,\lambda_0)\ .$$

The first two characteristics can be used to invert the parameterization, that is, to construct a map $(x,\lambda)\mapsto\tau$ and the *constant* $g(x_0,\lambda_0)$ is the initial data. The τ map, corresponds to the time it takes for a point $(x_0,\lambda_0)\in\mathcal{S}$ to *travel* to an arbitrary point $(x,\lambda)\in\mathbb{R}^2$ under the action of the flow of (7), can be solved explicitly as followed.

For some initial point (x_0,λ_0), the unique trajectory of this system evolve on the line $H^\star(x,\lambda)=H^\star(x_0,\lambda_0)$. Solving for λ, we have

$$\lambda(x)=2(-x^3\pm\sqrt{x^6+x^2-c})\ , \quad (18)$$

with the shorthand $c=H^\star(x_0,\lambda_0)$. The x-dynamics are given by

$$\frac{\mathrm{d}x}{\mathrm{d}\tau}=-x^3-\frac{1}{2}\lambda\overset{(18)}{=}\sigma\sqrt{x(\tau)^6+x(\tau)^2-c}\,,$$

where $\sigma=-\operatorname{sgn}(\lambda+2x^3)$.

Before we consider each partition separately, let's have a closer look at the indefinite integral for $c\neq 0$

$$\begin{aligned}\int\frac{\mathrm{d}x}{\sqrt{x^6+x^2-c}} &= \int\frac{\mathrm{d}z}{2\sqrt{z(z-\beta)(z-\alpha)(z-\gamma)}}\\ &= \frac{-\operatorname{sgn}(c)}{\sqrt{\gamma(\beta-\alpha)}}G(m(x),k)\ ,\end{aligned}$$

with $k,m(x),\alpha,\beta,\gamma,G$ stated in Section V.

a) On $\mathcal{H}_+$: The lines $H^\star(x,\lambda)=c$ intersects $\mathcal{S}$ at the point $(\operatorname{sgn}(x)\sqrt{c},0)$. By separation of variables we have that the time to travel from the point $\operatorname{sgn}(x)\sqrt{c}$ to the point x along the dynamics is given by

$$\tau=\sigma\int_{\operatorname{sgn}(x)\sqrt{c}}^{x}\frac{\mathrm{d}s}{\sqrt{s^6+s^2-c}}=-\sigma\left.\frac{G(m(z),k)}{\sqrt{\gamma(\beta-\alpha)}}\right|_{\operatorname{sgn}(x)\sqrt{c}}^{x}\ .$$

b) On $\mathcal{H}_-$: Trajectories intersect $\mathcal{S}$ at the points $(0,\operatorname{sgn}(x)2\sqrt{-c})$. A similar analysis yields

$$\tau=\sigma\int_0^x\frac{\mathrm{d}s}{\sqrt{s^6+s^2-c}}=\sigma\frac{G(m(x),k)}{\sqrt{\gamma(\beta-\alpha)}},$$

recalling that $m(0)=0$ and $G(0,k)=0$ for all $k\in(0,1)$.

c) On $\mathcal{H}_0$: Trajectories evolving on this manifold intersect with $\mathcal{S}$ only at the origin. But, since this point is an equilibrium of the system, special considerations are needed. Notice first that we have $c=0$, so the τ map is given by

$$\tau=\sigma\int_0^x\frac{\mathrm{d}s}{\sqrt{s^6+s^2}}\ .$$

But, the integral on the right-hand side does not converge on any interval containing zero. Looking at the indefinite integral

$$\int\frac{\mathrm{d}x}{\sqrt{x^6+x^2}}=-\frac{\operatorname{sgn}(x)}{2}\coth^{-1}\left(\sqrt{x^4+1}\right),$$

we have, for $H^\star(x,\lambda)=0$,

$$\tau=\frac{\operatorname{sgn}(x\lambda)}{2}\lim_{a\to 0}\coth^{-1}\left(\sqrt{z^4+1}\right)\Big|_a^x$$

the sign change comes from the fact that on $\mathcal{H}_0$, we have $\operatorname{sgn}(\lambda+x^3)=\operatorname{sgn}(\lambda)$ since $\lambda(\lambda+x^3)=2x^2+\frac{\lambda^2}{2}>0$. The result follows after collecting all the expressions for τ. ∎